frontiers

Supplementary Material: Superconductivity and its enhancement in polycyclic aromatic hydrocarbons

1 CRYSTAL AND ELECTRONIC STRUCTURES OF PRISTINE AND POTASSIUM-DOPED BENZENE

For pristine and K-doped benzene ($K_xC_6H_6$), the optimized crystal lattice constants and atomic coordinates are listed in Table S1. Solid benzene has rich phase diagram (Kozhin and Kitaigorodskii, 1955; Thiéry and Léger, 1988; Ciabini et al., 2007; Wen et al., 2011; Cox et al., 1958; Ciabini et al., 2005; Katrusiak et al., 2010; Fitzgibbons et al., 2015). Solid benzene is a wide band gap insulator as shown in Figure S1A. Our calculated band gap of 4.1 eV is in a good agreement with the previous result4. Since there are four inequivalent benzene molecules in benzene crystal, the highest occupied molecular orbitals (HOMO) of the benzene molecules hybridize, which gives rise to four partly degenerated bands just below the Fermi level. The first group of valence band together with four partly degenerated bands originating from HOMO-1's is thus formed. Similarly, the hybridization between the lowest unoccupied molecular orbitals (LUMO) and LUMO+1 produces four partly degenerated bands in the range of $4.1 - 5.2$ eV. These eight bands as shown in Figure S1B, forming the first group of conduction bands, are marked by CB1, CB2, CB3, ..., and CB8 in the energy ordering from low to high, respectively.

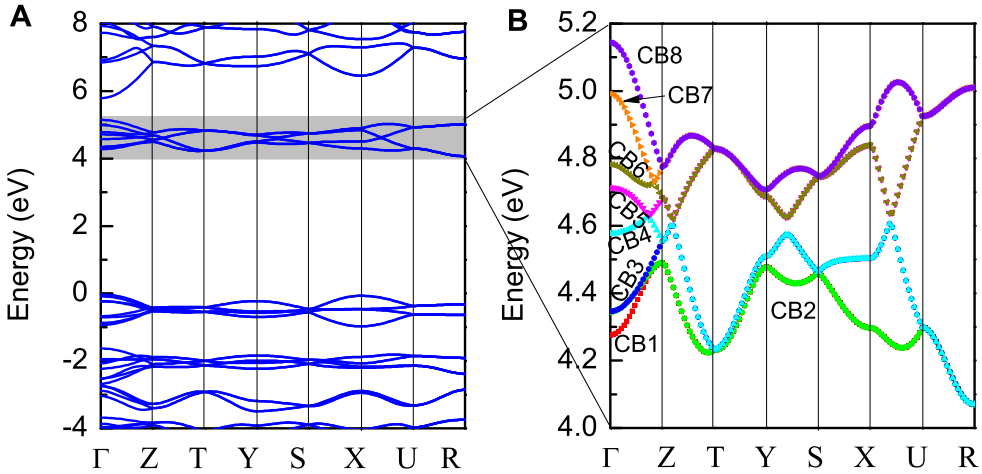

Figure S1. Band structures of solid benzene. **(A)**, Calculated band structures along high symmetrical k-point directions in Brillouin zone. **(B)**, Zoom in the range of 4.0-5.2 eV. Zero energy denotes the Fermi level.

Table S1. Optimized crystal lattice constants and atomic coordinates for pristine and K-doped benzene.

System	a (Å)	b (Å)	c (Å)	Atom	Coordinates x	y	z
C_6H_6	7.041	8.903	6.357	C1	0.93225	0.14642	0.99416
				C2	0.85349	0.04372	0.13328
				C3	0.92184	0.89756	0.13897
				H1	0.12079	0.76234	0.51082
				H2	0.26345	0.57627	0.26184
				H3	0.63912	0.31717	0.25078
$K_1C_6H_6$	7.038	10.153	6.954	C1	0.99905	0.13688	0.00054
				C2	0.87487	0.07037	0.12201
				C3	0.87575	0.92834	0.12147
				H1	0.00191	0.74496	0.49898
				H2	0.22108	0.62599	0.28286
				H3	0.71963	0.37179	0.21598
				K	0	0	0.5
$K_2C_6H_6$	8.605	10.705	6.415	C1	0.00025	0.13112	0.50003
				C2	0.99999	0.06715	0.69116
				C3	0.99980	0.93280	0.69114
				H1	0.99945	0.73266	0.99989
				H2	0.99994	0.62289	0.66622
				H3	0.50027	0.37707	0.83378
				K	0.27354	0.50011	0.00010
$K_3C_6H_6$	8.537	8.496	8.273	C1	0.96985	0.12518	0.88945
				C2	0.86021	0.10103	0.02305
				C3	0.90174	0.97697	0.13737
				H1	0.05886	0.71408	0.70363
				H2	0.19348	0.70986	0.42587
				H3	0.67962	0.44984	0.23773
				K1	0.16992	0.32978	0.66196
				K2	0	0	0

2 STABILITY OF K-DOPED BENZENE

The formation energy (E_f) is good indication for examining the stability. $E_f < 0$ indicates that the doped compound can stably exist. Figure S2 presents the dependence of formation energy on chemical potential of K for different doped phases. In certain a region of chemical potential, $K_2C_6H_6$ has lower formation energy than $K_1C_6H_6$, $K_{2.5}C_6H_6$ and $K_3C_6H_6$. And the negative sign of formation energy suggests easier synthesization of $K_2C_6H_6$ phase.

3 COMPARISON OF GEOMETRICAL STRUCTURE AND SUPERCONDUCTIVITY BETWEEN THE $K_2C_6H_6$ AND THE INTERCALATED GRAPHITE COMPOUNDS C_6M

In geometrical structure, as shown in Figure S3, the K metal intercalated $K_2C_6H_6$ has the similar characteristics to the intercalated graphite compounds C_6M (M =Yb, Ca). Both are the layered configuration. There is the comparable superconductivity between $K_2C_6H_6$ and C_6Yb, especially for between $K_2C_6H_6$ and C_6M, with $T_c \sim 6$ K.

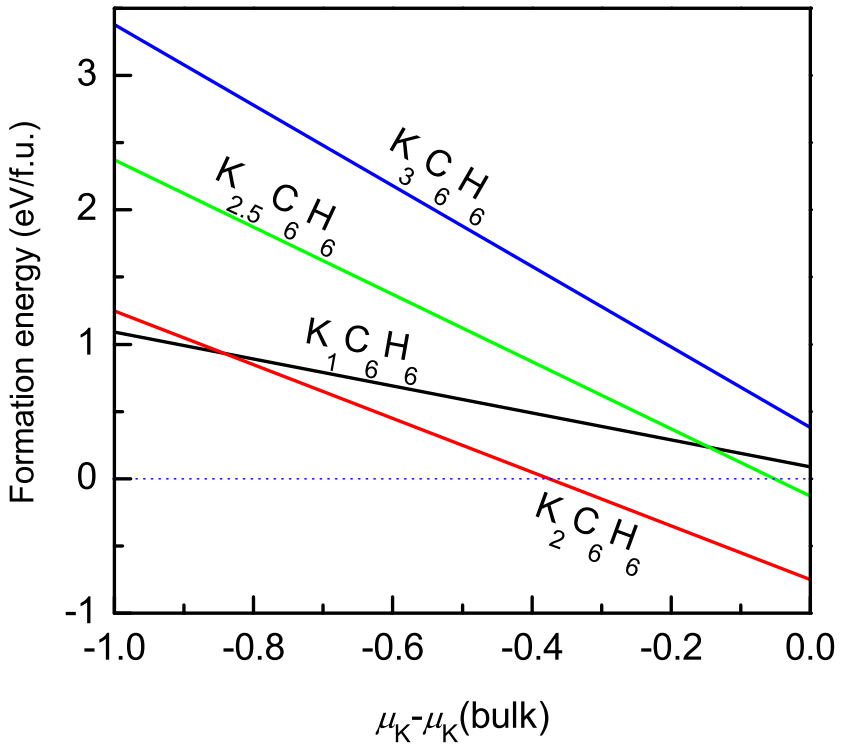

Figure S2. Stability of K-doped benzene. Formation energy of K-doped benzene as a function of the K chemical potential. μ_K(bulk) can be obtained from the energy per K atom in its pure element phase, e.g., K metal with the *bcc* structure. $\mu_K = \mu_K$(bulk) means the element is so rich that the pure element phase can form.

4 CRYSTAL STRUCTURES AND STABILITIES OF POTASSIUM-DOPED NAPHTHALENE

As a supplement, we have studied the solid naphthalene ($C_{10}H_8$) to investigate whether the K-doped $C_{10}H_8$ is superconducting. Three doping concentrations were considered, namely $K_xC_{10}H_8$ (x = 1, 2, and 3). The optimized structures with $P2_1/a$ symmetry are shown in Figure S4, and the lattice parameters are listed in Table S2. To check the stability, the formation energy was calculated, as shown in Figure S5. In K-rich region, the formation energies of doped $C_{10}H_8$ are negative, especially for $K_1C_{10}H_8$ and $K_2C_{10}H_8$, which means that these three compounds can be obtained experimentally. But $K_2C_{10}H_8$ is the most stable in this series and easy to be fabricated experimentally.

5 ELECTRONIC STRUCTURES OF PRISTINE AND POTASSIUM-DOPED NAPHTHALENE

The electronic band structures shown in Figure S6 indicate the doped naphthalene is metal as $x = 1$ or 3. However, $K_2C_{10}H_8$ exhibits the absence of metallic character, with a band gap about 0.75 eV which is larger than 0.19 eV of $K_2C_{22}H_{14}$.

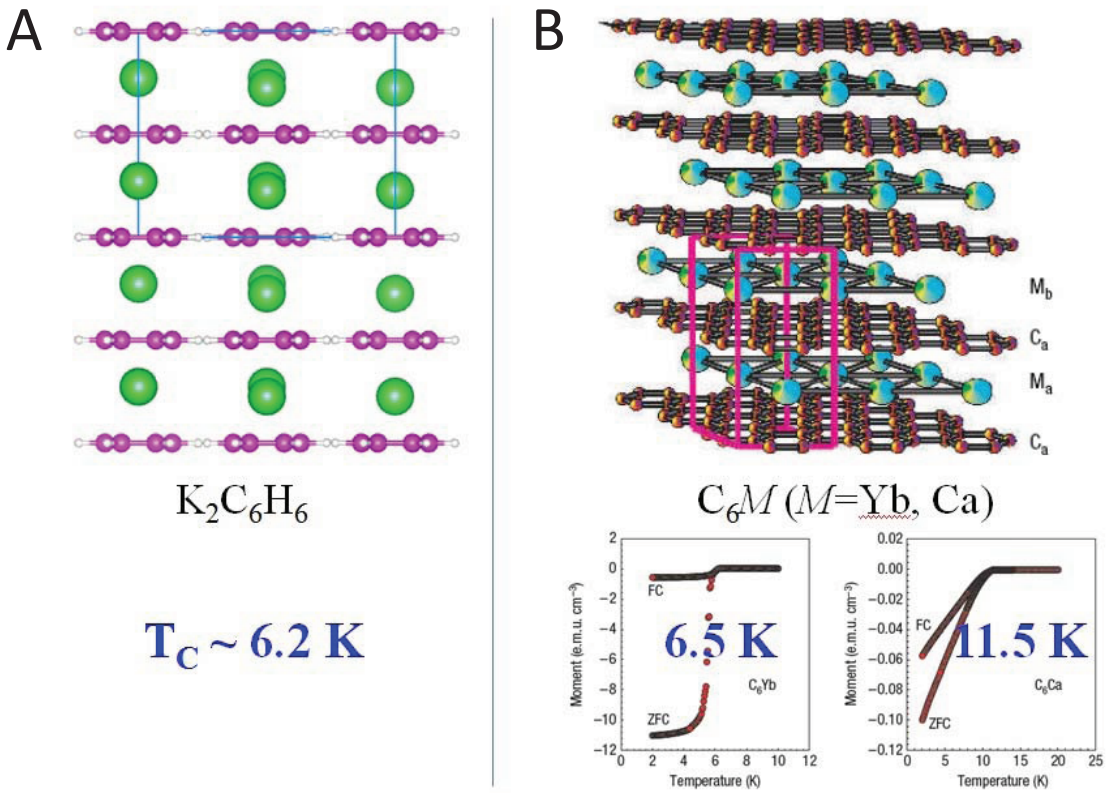

Figure S3. Comparison of geometrical structure and superconductivity. **(A)**, Optimized crystal structure of $K_2C_6H_6$ with the layer feature and superconducting critical temperature T_c. **(B)**, Structure of the intercalated graphite compounds C_6M (M =Yb, Ca) and measurements of the magnetization. (Weller et al., 2005; Emery et al., 2005)

Table S2. Optimized crystal lattice parameters for pristine and K-doped naphthalene. The experimental values are taken from Ref. 11.

System	a (Å)	b (Å)	c (Å)	β (°)	V (Å^3)
$C_{10}H_8$ (Ref.11)	8.235	6.003	8.658	122.92	359.3
$C_{10}H_8$	8.221	5.904	8.550	123.10	347.6
$K_1C_{10}H_8$	8.658	7.215	8.822	133.02	402.9
$K_2C_{10}H_8$	7.672	7.350	8.613	115.75	438.1
$(K_2C_{10}H_8)^{+0.1e}$	7.719	7.401	8.674	115.86	445.9
$(K_2C_{10}H_8)^{-0.1e}$	7.690	7.322	8.442	115.37	429.5
$K_3C_{10}H_8$	7.678	7.376	12.505	112.62	653.7

6 COMPARISON OF POTASSIUM-DOPED NAPHTHALENE AND PICENE WITH CHARGE FLUCTUATIONS

For this situation of potassium-doped picene $K_2C_{22}H_{14}$, we examined the possibility of local metallization. Introducing a small quantity of charge into $K_2C_{22}H_{14}$, the calculated results showed in Figure S7 indicate that $(K_2C_{22}H_{14})^{+0.1e}$ becomes to metal from narrow semiconductor. For $(K_2C_{10}H_8)^{\pm 0.1e}$ with the same charge, we calculated their band structures. As shown in Figure S8, $(K_2C_{10}H_8)^{\pm 0.1e}$ with a small amount of charge fluctuations just become to metal from semiconductor.

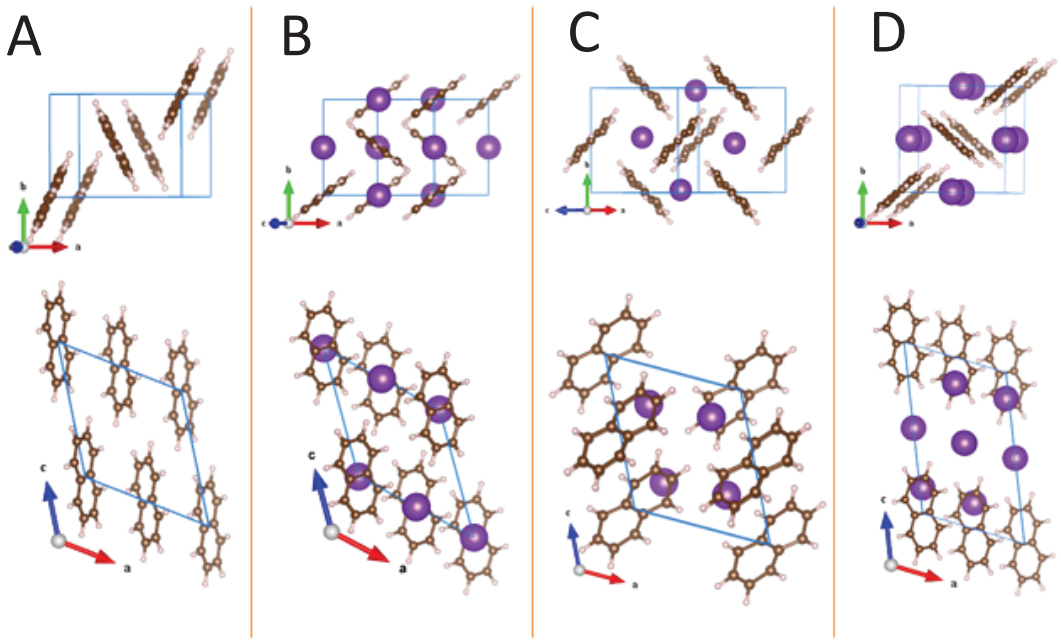

Figure S4. Structures of potassium-doped naphthalene ($K_xC_{10}H_8$, $x = 1, 2, 3$) comparing with undoped case. **(A)**,$C_{10}H_8$; **(B)**, $K_1C_{10}H_8$; **(C)**, $K_2C_{10}H_8$; **(D)**, $K_3C_{10}H_8$. The purple balls represent K atoms.

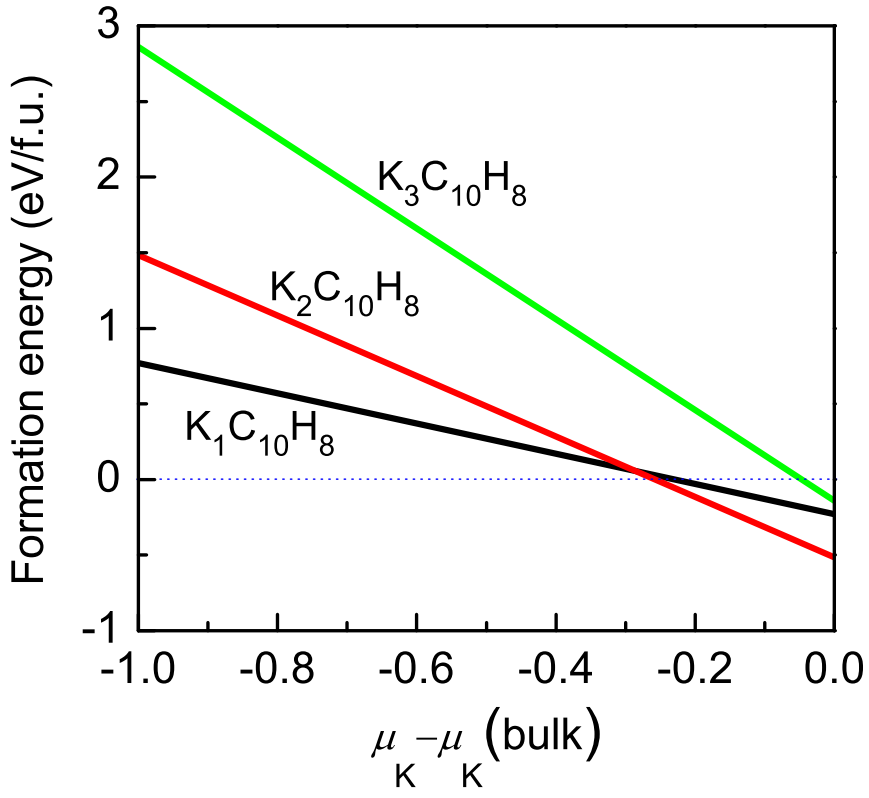

Figure S5. Stability analysis of potassium-doped naphthalene ($K_xC_{10}H_8$). Formation energy of K-doped naphthalene as a function of the K chemical potential.

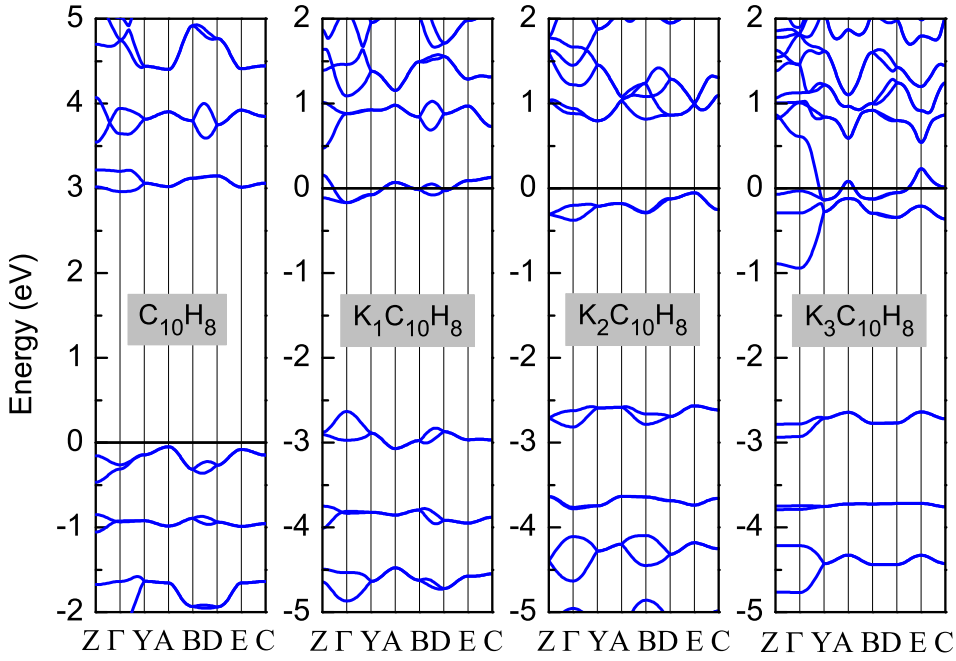

Figure S6. Variations of band structures of potassium-doped naphthalene with the change of the doping levels. Calculated band structures of $C_{10}H_8$ and $K_xC_{10}H_8$ (x = 1, 2, and 3). Zero energy denotes the Fermi level.

7 ELECTRON-PHONON COUPLING AND T_C ESTIMATING OF CHARGED $K_2C_{10}H_8$.

For metallic $(K_2C_{10}H_8)^{+0.1e}$, the electron-phonon interaction was calculated. Figure S9 presents the Eliashberg spectral function $\alpha^2F(\omega)$ (left axis) and the electron-phonon coupling integral $\lambda(\omega)$ (right axis). We obtain the electron-phonon coupling constant $\lambda = 0.64$ and the logarithmic average of phonon frequencies $\omega_{log} = 210.4$ K. Thus, we can estimate the T_c as 5.8 K with the help of the modified McMillan equation of Allen and Dynes. The results on doped naphthalene have the similarities with those of doped benzene.

8 A COMPARISON OF THE PREDICTED SUPERCONDUCTIVITIES OF BENZENE, NAPHTHALENE AND PHENANTHRENE WITH PICENE ESTIMATED BY CASULA ET AL. (Casula et al., 2011)

We here present our predicted superconductivity of benzene, naphthalene and phenanthrene ($C_{14}H_{10}$) comparing with picene ($C_{22}H_{14}$) estimated by Casula et al. (**?**) in the electron-phonon coupling Eliashberg spectral function $\alpha^2F(\omega)$ and the electron-phonon coupling integral $\lambda(\omega)$, as shown in Figure S10. And the calculated superconduction parameters of λ, ω_{log} and T_c are summarized in Table S3. From the comparison, the superconducting parameters possess the similarity in quantity. This comes mainly from the comparable DOS values at the Fermi level for these systems.

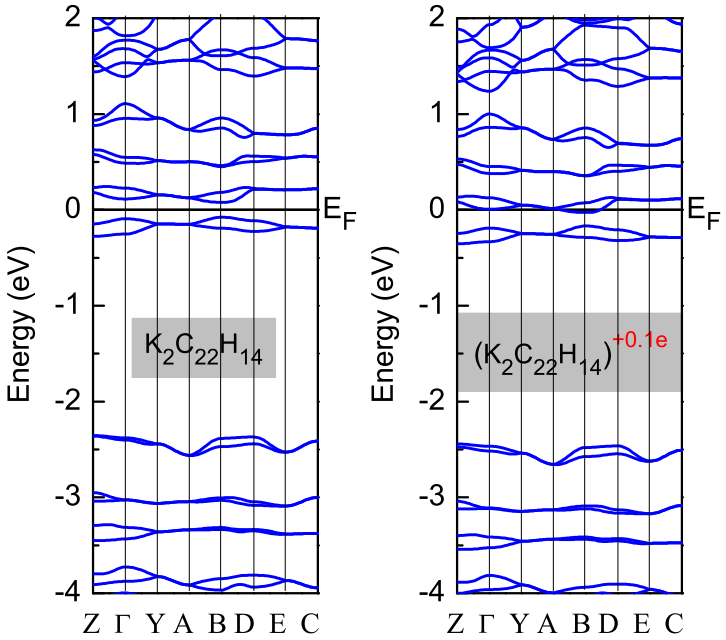

Figure S7. Variations of band structures of K_2picene induced by the charge fluctuations. Comparison of band structures of $K_2C_{22}H_{14}$ and charged $(K_2C_{22}H_{14})^{+0.1e}$. Zero energy denotes the Fermi level.

Table S3. Comparisons of superconduction parameters of K-doped benzene, naphthalene, phenanthrene and picene.

	$K_2C_6H_6$	$(K_2C_{10}H_8)^{+0.1e}$	$K_2C_{14}H_{10}$	$K_3C_{22}H_{14}$ (Ref. 12)
λ	0.67	6.4	0.58	0.73
ω_{log} (K)	199.8	210.4	193.7	207
$T_c(K)(\mu^\star = 0.1)$	6.2	5.8	3.9	8

9 STABILITIES OF K-DOPED ALL CONSIDERED AROMATIC HYDROCARBONS

Here, in Figure S11, we present the formation energy as a function of the K chemical potential for K-doped benzene, naphthalene, phenanthrene and chrysene ($K_xC_{18}H_{12}$). For these four systems with short-benzene-ring chain, there is a common feature of that K_2-doping is the most stable in the region of K chemical potential satisfying the formation energy less than zero. In Figure S12, we show the formation energy as a function of the K chemical potential for K-doped picene, [6]phenacene ($C_{26}H_{16}$) and 1,2;8,9-dibenzopentacene ($C_{30}H_{18}$). For these three systems with long-benzene-ring chain, both the dopings of two and three electrons are respectively the most stable phase in the different region of K chemical potential. Stable multi-doping phases can coexist in long-benzene-ring systems. However, in all aromatic hydrocarbons, it is a common feature that the doping of two electrons is stable.

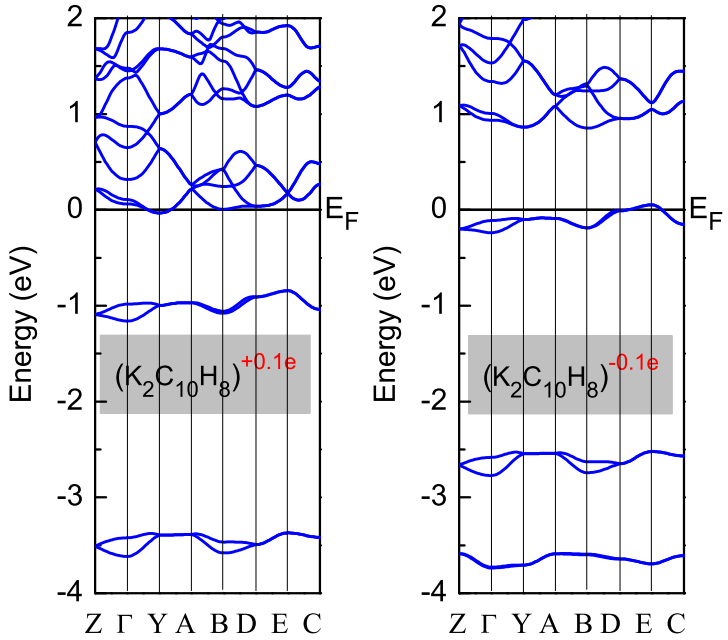

Figure S8. Variations of band structures of K_2naphthalene induced by the charge fluctuations. Comparison of band structures of charged $(K_2C_{10}H_8)^{+0.1e}$ and $(K_2C_{10}H_8)^{-0.1e}$. Zero energy denotes the Fermi level.

10 ELECTRON-ELECTRON CORRELATIONS IN HYDROCARBON SUPERCONDUCTORS

We have estimated the electron correlations. We calculated the on-site inter-electron repulsion U_{bare} for a single molecule with three electrons from the energies of the molecule charged with 2, 3, and 4 electrons as $U_{bare} = E(2)+E(4)-2E(3)$, where $E(Z)$ is the total energy of a molecule charged with Z extra electrons. Such an estimate for an isolated molecule needs to be corrected by $E_{pol}(Z)$ to reflect the screening effects in the solid. The effect of the polarization of a charged molecule placed inside a cavity of a homogeneous dielectric medium characterized by a dielectric constant ε is thus considered to determine the effective repulsion $U_{eff} = U_{bare}-E_{pol}$. As a result, the parameter U_{eff}/W can be used to determine the magnitude of electronic correlation effects, where W is the width of bands crossing the Fermi level. The calculated results imply an enhancement of electronic correlation effects with the increase of the number of benzene rings.

REFERENCES

Casula, M., Calandra, M., Profeta, G., and Mauri, F. (2011). Intercalant and intermolecular phonon assisted superconductivity in k-doped picene. *Phys Rev Lett* 107, 137006. doi:10.1103/PhysRevLett.107.137006

Ciabini, L., Gorelli, F., Santoro, M., Bini, R., Schettino, V., and Mezouar, M. (2005). High-pressure and high-temperature equation of state and phase diagram of solid benzene. *Phys Rev B* 72, 094108.

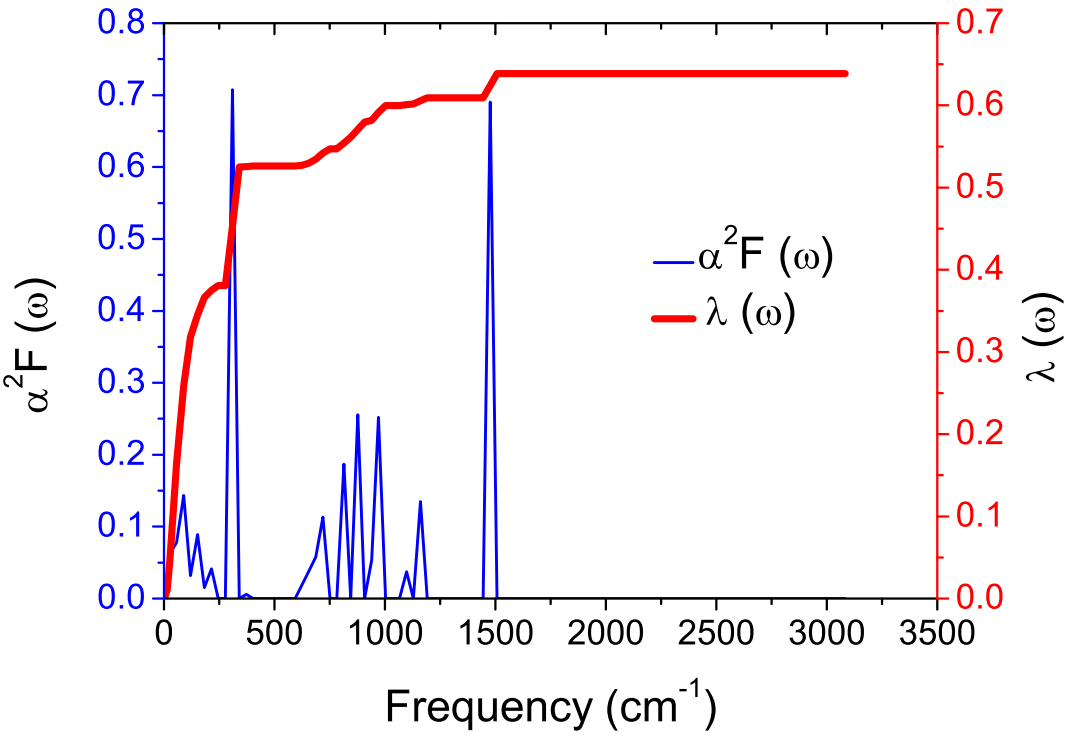

Figure S9. Electron-phonon coupling of K-doped benzene. Electron-phonon coupling Eliashberg spectral function $\alpha^2F(\omega)$ (left axis) and the electron-phonon coupling integral $\lambda(\omega)$ (right axis) of $(K_2C_{10}H_8)^{+0.1e}$.

doi:10.1103/PhysRevB.72.094108

Ciabini, L., Santoro, M., Gorelli, F., Bini, R., Schettino, V., and Raugei, S. (2007). Triggering dynamics of the high-pressure benzene amorphization. *Nature Mater* 6, 39–43. doi:10.1038/nmat1803

Cox, E., Cruickshank, D., and Smith, J. (1958). The crystal structure of benzene at -3 °c. *Proc R Soc Lond A* 247, 1–20

Emery, N., Hérold, C., d'Astuto, M., Garcia, V., Bellin, C., Marêché, J., et al. (2005). Superconductivity of bulk cac$_6$. *Phys Rev Lett* 95, 087003. doi:10.1103/PhysRevLett.95.087003

Fitzgibbons, T., Guthrie, M., s Xu, E., Crespi, V., Davidowski, S., Cody, G., et al. (2015). Superconductivity at 14.2 k in layered organics under extreme pressure. *Nature Mater. DOI: 10.1038/NMAT4088 (2014).* 14, 43–47. doi:10.1038/NMAT4088

Katrusiak, A., Podsiadlo, M., and Budzianowski, A. (2010). Association ch...π and no van der waals contacts at the lowest limits of crystalline benzene i and ii stability regions. *Cryst Growth Des* 10, 3461–3465. doi:10.1021/cg1002594

Kozhin, V. and Kitaigorodskii, A. (1955). Nizkotemperaturnye issledovaniya struktury aromaticheskikh soedinenii. 4. anizotropiya teplovogo rasshireniya v benzole. *Zh Fiz Khim* 29, 2074–2075

Thiéry, M. and Léger, J. (1988). High-pressure solid-phases of benzene. 1. raman and x-ray studies of c$_6$h$_6$ at 294 k up to 25 gpa. *J Chem Phys* 89, 4255–4271. doi:10.1063/1.454809

Weller, T., Ellerby, M., Saxena, S., Smith, P., and Skipper, N. (2005). Superconductivity in the intercalated graphite compounds c$_6$yb and c$_6$ca. *Nat Phys* 1, 39–41. doi:10.1038/nphys0010

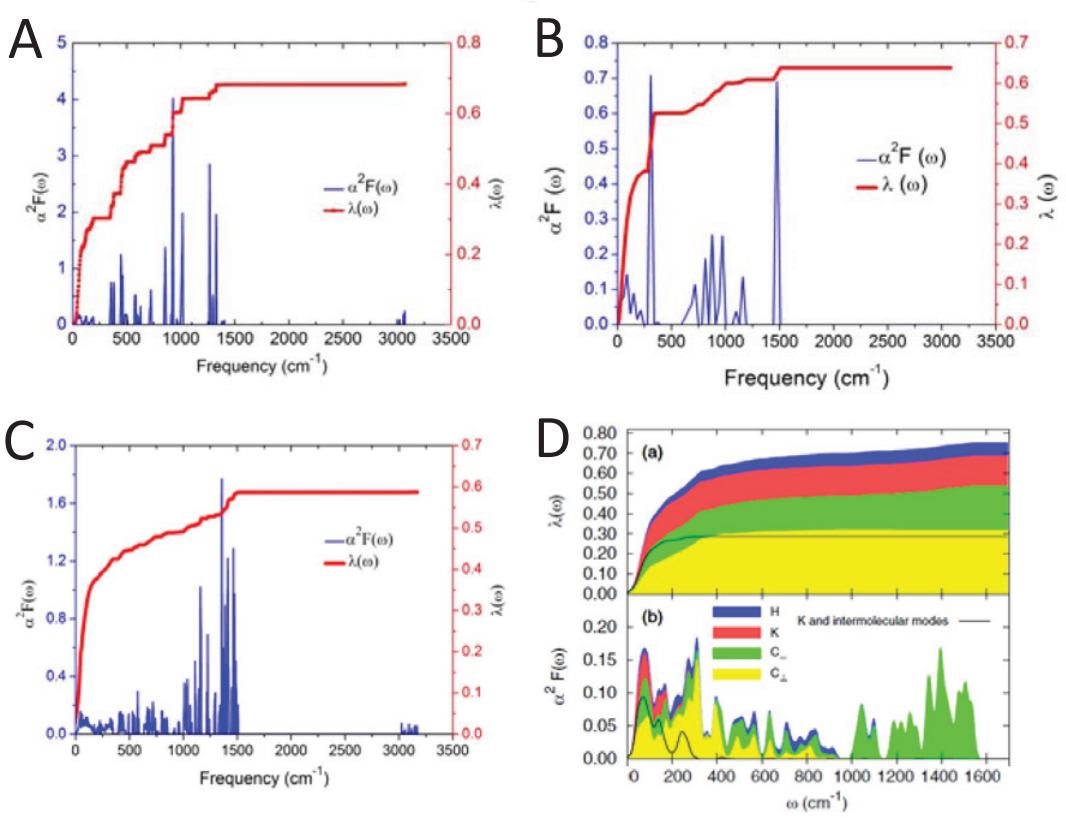

Figure S10. A comparison of the predicted superconductivities in benzene, naphthalene and phenanthrene with picene estimated by Casula et al. (**?**) The electron-phonon coupling Eliashberg spectral function $\alpha^2F(\omega)$ and the electron-phonon coupling integral $\lambda(\omega)$ of $K_2C_6H_6$ **(A)**, $K_2C_{10}H_8$ **(B)**, $K_2C_{14}H_{10}$ **(C)** and $K_3C_{22}H_{14}$ **(D)** in Ref 12.

Wen, X., Hoffmann, R., and Ashcroft, N. (2011). Benzene under high pressure: a story of molecular crystals transforming to saturated networks, with a possible intermediate metallic phase. *J Am Chem Soc* 13, 9023–9035. doi:10.1021/ja201786y

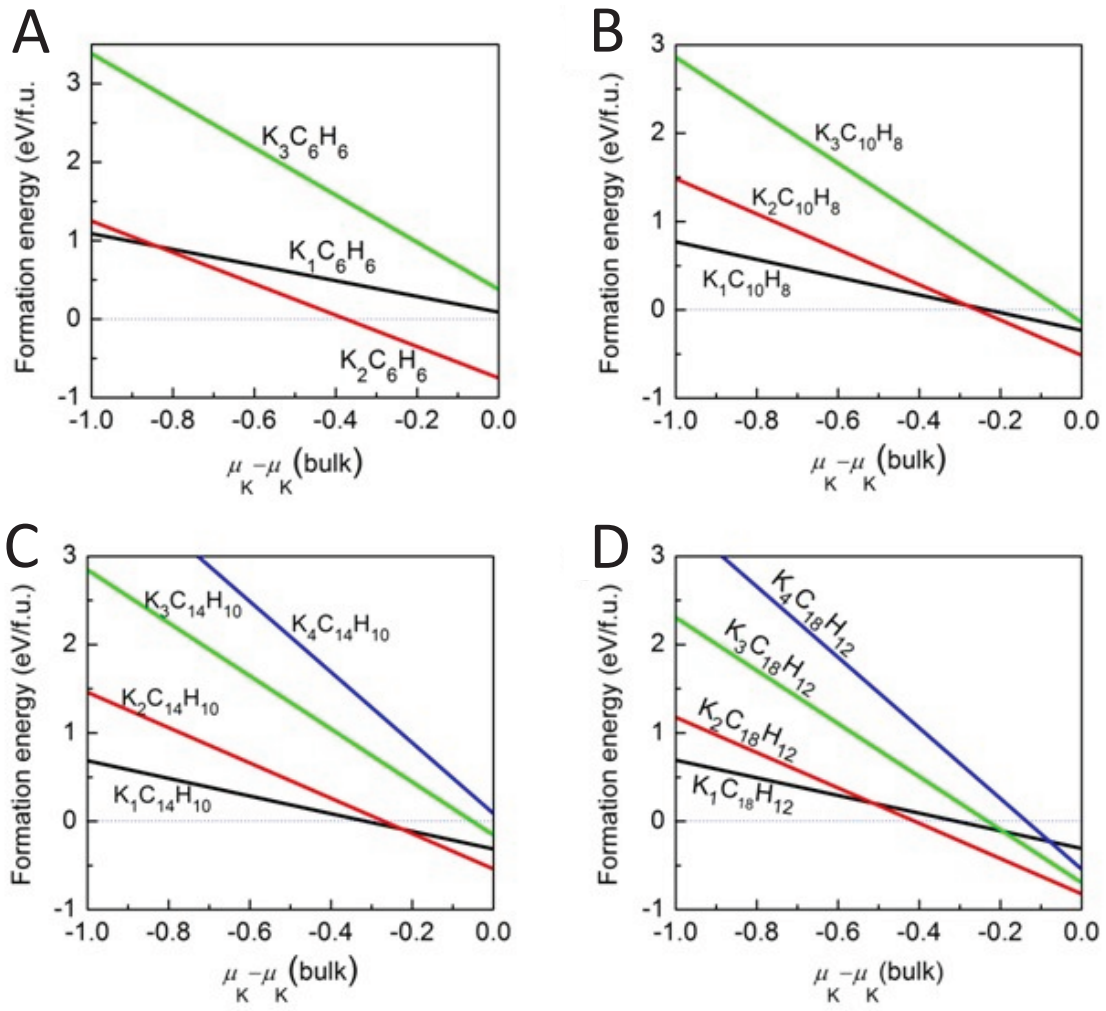

Figure S11. Stability analysis of K-doped aromatic hydrocarbons with the short-benzene-ring chain. Formation energy of K-doped benzene, naphthalene, phenanthrene and chrysene as a function of the K chemical potential. ***(A)***, $K_xC_6H_6$; **(B)**, $K_xC_{10}H_8$; **(C)**, $K_xC_{14}H_{10}$; **(D)**, $K_xC_{18}H_{12}$.

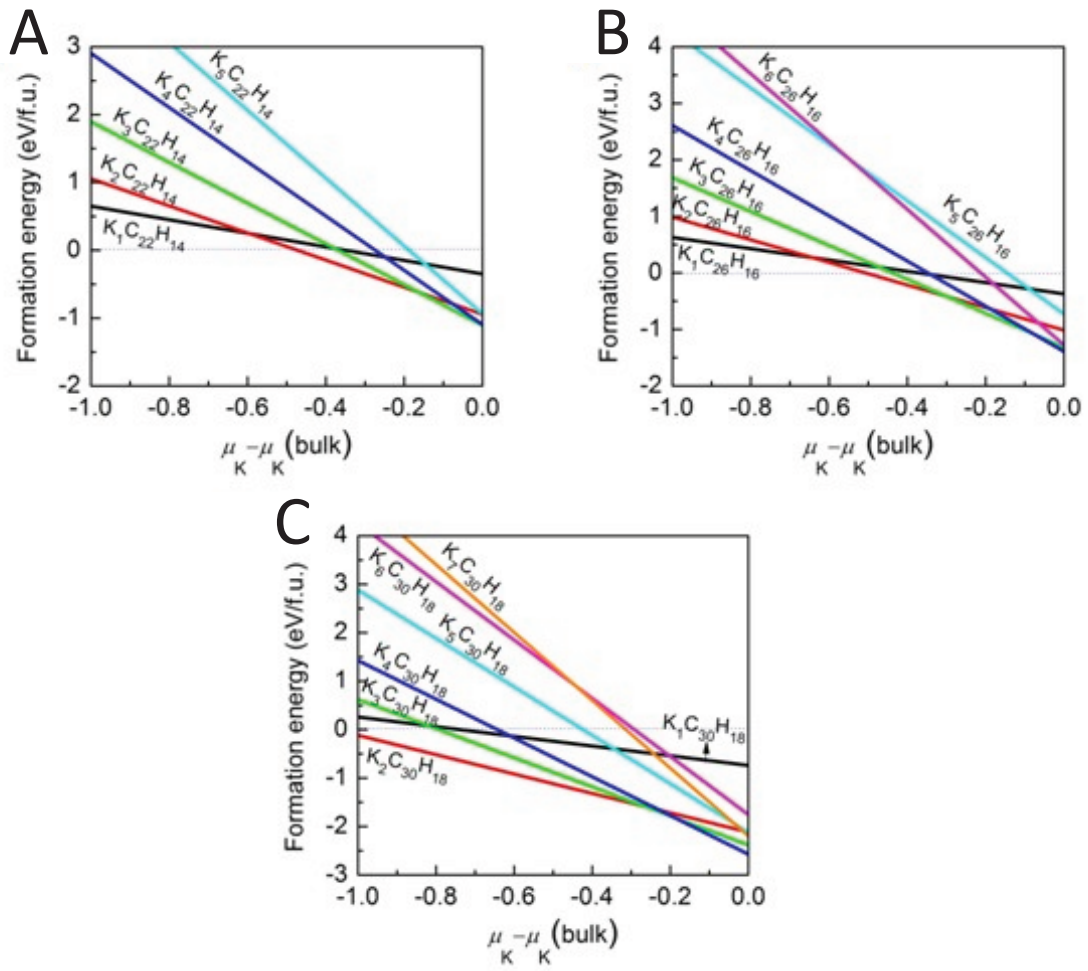

Figure S12. Stability analysis of K-doped aromatic hydrocarbons with the long-benzene-ring chain. Formation energy of K-doped picene, [6]phenacene ($C_{26}H_{16}$) and 1,2;8,9-dibenzopentacene ($C_{30}H_{18}$) as a function of the K chemical potential. **(A)**, $K_xC_{22}H_{14}$; **(B)**, $K_xC_{26}H_{16}$; **(C)**, $K_xC_{30}H_{18}$.